NUCLEAR ENGINEERING AND TECHNOLOGY
ISSN / eISSN 1738-5733
Publisher KOREAN NUCLEAR SOC,
NUTOPIA BLDG, 342-1 JANGDAE-DONG,
DAEJEON, SOUTH KOREA, 305-308
Volume 26 -Issue 1-(2026)
DOI:https://doi.org/10.65281/736343

OPEN ACCESS

Synergistic effect of saline environment and hydrogen peroxide on the mechanical integrity of AISI 304 stainless steel surgical instruments

Check for updates

Lazhar Yahia [1,2,*], Fatima Zohra Benlahreche [3], ZIDANI Sara [4],BAIRA Fayçal [5]

[1]Department of Electromechanical Engineering, Faculty of Technology, University of Batna 2, Batna 05000, Algeria.

Email: l.yahiar@univ-batna2.dz; Orcid: 0009-0004-8996-4320

[2]Surface Engineering Laboratory, Department of Chemistry**,** Faculty of Sciences, University of Annaba, Annaba 23000, Algeria.

[3]Department of Chemical Engineering, Faculty of Process Engineering, University of Constantine 3, 25000, Algeria.

Email: fatima.benlahreche@univ-constantine3.dz; Orcid: 0009-0009-3473-7872

[4] university of Batna Departement of Food Technology, laboratory of Food Science (lSa), institute of veterinary and agricultural Sciences, 1 hadjlakhdar, alleys may 19 Biskra avenue, Batna, 05000, Algeria

Email: sara.zidani@univ-batna.dz ; Orcid: 0009-0004-3604-2437

[5] university of Batna 2, Faculty of Technology, Department oF Sciences and Technology, alleys 53, constantine avenue. Fésdis, Batna 05078, Algeria

Email: f.baira@univ-batna2.dz ; 0009-0008-0869-8614

E-mail: l.yahiar@univ-batna2.dz

Received : 20/02/2026 ; Accepted : 27/05/2026

Abstract

This study investigates the synergistic effects of saline physiological environments (3.5% NaCl) and hydrogen peroxide (H_2O_2) sterilization agents on the mechanical integrity of AISI 304 austenitic stainless steel, a gold standard for critical surgical instrumentation requiring high corrosion resistance. To simulate aggressive clinical conditions and repeated chemical sterilization cycles, uniaxial tensile tests were performed at a controlled human body temperature of 37 °C, complemented by microstructural characterization. Experimental results demonstrate that while the ultimate tensile strength remains stable, the yield strength, critical for surgical tool precision, exhibits significant degradation in peroxide-enriched saline media. Notably, specific H_2O_2 concentrations led to a stabilization in fracture stress and elongation, identifying a clinical safety threshold for ductility loss. This research quantifies the vulnerability of the AISI 304 elastic limit under combined bio-chemical exposure, providing vital data for the life-cycle assessment and structural reliability of reusable medical devices subjected to harsh disinfection protocols.

Keywords: AISI 304 stainless steel, surgical instrumentation, hydrogen peroxide (H_2O_2), sodium chloride (NaCl), mechanical degradation, yield strength.

1. Introduction

The strategic significance of austenitic stainless steels, particularly the AISI 304 grade, is paramount in modern healthcare infrastructure. Their ubiquitous application in critical medical sectors, ranging from high-precision surgical instrumentation to orthopedic fixation devices, is attributed to a unique combination of high ductility and intrinsic resistance to corrosion [1–5]. This chemical stability originates from a self-healing passive film, predominantly composed of chromium oxide (Cr_2O_3), serving as a potent kinetic barrier against environmental degradation. Despite these advantages, operational environments in clinical settings often impose severe thermochemical constraints, particularly during repeated chemical sterilization cycles, leading to the localized breakdown of this protective layer [6–8].

The motivation for this present scientific research stems from the increasing structural reliability issues encountered in reusable medical devices. Recent investigations highlight that mechanical processing and residual stress distributions significantly alter passivity. Notably, it has been demonstrated that deformation plays a critical role in the corrosion kinetics of 304 stainless steel in chloride media [9-11]. This susceptibility is further intensified by potent oxidizing agents such as hydrogen peroxide (H_2O_2), widely used in modern sterilization, which can accelerate ionic diffusion through the passive scale [12, 13].

The relevance of the present work lies in its systematic evaluation of the synergistic effects of sodium chloride (NaCl) and hydrogen peroxide (H_2O_2) on high-precision components. Pitting corrosion generates discrete geometric discontinuities that function as potent stress concentrators [14, 15]. Exposure to such harsh biochemical media, especially at the 37 °C threshold of the human body, can induce a deleterious shift in the material's constitutive law [17], characterized by a significant loss in yield strength as observed in simulated physiological environments [16].

The border impact of this study is significant for the current medical scenario, as it provides essential data for enhancing predictive maintenance models and structural safety margins for surgical instruments. By simulating specific oxidative-saline sterilization environments, this research offers a direct correlation between chemical aggressiveness and the resulting elastoplastic behaviour, facilitating the design of more resilient medical components and ensuring patient safety throughout the devices' operational life-cycle.

2. Experimental procedure

2.1. Material

The experimental investigation was performed on AISI 304 austenitic stainless steel (UNS S30400), a medical-grade alloy widely utilized in the production of high-precision surgical instruments. The raw material was sourced from the BCR National Enterprise (Bolts, Cutlery, and Fittings) located in Bordj-Menaiel, Algeria. This specific grade was selected due to its extensive use in the manufacturing of reusable medical devices, such as forceps and scalpels, which require a critical balance of mechanical toughness, sterilization resistance, and electrochemical stability [18].

The metallurgical integrity of this alloy is governed by its stable face-centered cubic (FCC) austenitic lattice structure, ensuring high fracture toughness and superior ductility under severe clinical loading conditions. While the material is essentially non-magnetic in its fully annealed state, the complex machining and cold-working processes required to shape surgical tools can trigger a

partial phase transformation into strain-induced α′ martensite. This microstructural evolution is of paramount importance for medical applications, as it modifies the magnetic signature of the alloy, potentially affecting MRI compatibility, and creates preferential sites for localized pitting corrosion, thereby compromising the sterile service life of instruments operating in aggressive disinfecting media.

The chemical composition of the investigated alloy, adhering to ISO 7153-1 standards for surgical-grade stainless steels, is summarized in Table 1.

Table 1. Elemental composition of the investigated AISI 304 stainless steel (wt. %).

Element	Cr	Ni	Mn	Si	C	S	P	Fe
Wt.%	17.95	8.01	1.20	0.40	0.05	0.02	0.03	Balance

The precise balance of chromium (minimum 18%) and nickel (minimum 8%) ensures the rapid formation of a robust, self-healing passive Cr_2O_3 layer. Furthermore, the rigorous control of interstitial carbon concentration is vital to prevent chromium carbide precipitation at grain boundaries during any thermal treatment or welding process. This minimizes the risk of sensitization and intergranular corrosion, which are unacceptable in clinical environments.

The individual roles of the alloying elements in the AISI 304 matrix are fundamental to its macroscopic behavior and clinical reliability. Chromium (Cr), present at 17.95 wt.%, is the primary alloying element responsible for the formation of the dense protective passive film Cr_2O_3, which ensures exceptional resistance against oxidative and corrosive attacks during repeated chemical sterilization. Nickel (Ni), at 8.01 wt.%, acts as a powerful austenite stabilizer, maintaining the face-centered cubic (FCC) structure and enhancing the alloy's toughness and ductility, which are essential for the structural integrity of thin-walled surgical tools.

Manganese (Mn) and Silicon (Si) serve as deoxidizers during the melting process, with manganese also contributing to the stabilization of the austenitic phase and improving hot-working properties during the forging of instrument handles. The low Carbon (C) content (0.05 wt.%) is strategically maintained to minimize the risk of chromium carbide precipitation ($Cr_{23}C_6$) at grain boundaries, thereby preventing sensitization and intergranular corrosion, a critical requirement for maintaining a sterile surface. Finally, the restricted levels of Sulfur (S) and Magnesium (Mg) are essential to ensure the metallurgical cleanliness of the steel. By avoiding the formation of non-metallic inclusions, such as manganese sulfides (MnS), the material eliminates potential initiation sites for pitting corrosion in aggressive chloride-rich physiological media.

2.2. Specimen machining and geometry

Standardized cylindrical tensile specimens were precision-machined from 15 mm diameter AISI 304 rods to a final gauge diameter of 10 mm. The fabrication process was executed using a high-precision Computer Numerical Control (CNC) lathe at the Mechanical Construction Company of Khenchela (MCCK). To ensure superior surface integrity and prevent thermal alterations of the microstructure, the machining was performed under a continuous flow of a high-performance water-soluble cooling emulsion (synthetic cutting fluid).

The optimized CNC parameters combined with effective lubrication allowed for achieving a defect-free, mirror-like surface finish directly during the machining process, effectively eliminating the need for subsequent manual polishing. This advanced surface state was fundamental to suppress any micro-notches that could act as preferential sites for localized pitting. Finally, all dimensions and tolerances were metrologically verified to ensure rigorous compliance with ISO 6892-1 standards (Figure 1).

Figure 1. Geometry and dimensions of the standardized cylindrical tensile specimen machined by CNC according to ISO 6892-1.

2.3. Surface preparation

The surface integrity of the cylindrical specimens was strictly controlled to minimize the influence of machining-induced residual stresses on the corrosion-mechanical synergy. Owing to the high-precision CNC turning process, a defect-free, mirror-like finish was achieved directly on all active surfaces within the gauge length. This superior surface quality was essential to eliminate micro-notches that could act as premature pitting sites during aggressive chemical exposure.

To ensure the complete removal of residual cooling emulsions or contaminants, a rigorous cleaning protocol was applied. The specimens were degreased in an ultrasonic bath of acetone for 15 minutes, followed by rinsing with deionized water. Finally, the samples were carefully dried using a high-pressure air dryer to prevent atmospheric oxidation prior to their immediate immersion in the corrosive media.

2.4. Environmental exposure and immersion protocols

The primary objective of this experimental phase was to evaluate the mechanical integrity of AISI 304L stainless steel under aggressive conditions. This grade was specifically selected due to its widespread use in the manufacture of surgical instruments and medical devices. The experimental conditions were designed to simulate both physiological environments and harsh clinical sterilization cycles. Standardized cylindrical specimens were subjected to seven distinct immersion protocols, designated TR0 to TR06.

The corrosive medium for all batches consisted of a 3.5% NaCl saline solution, providing a constant source of chloride ions (Cl^-) to destabilize the Cr_2O_3 passive film through competitive adsorption and localized penetration. To simulate advanced oxidation processes (AOPs) and clinical disinfection environments where surgical tools are exposed to intense oxidative stress, hydrogen peroxide (H_2O_2) was integrated as a potent oxidizing agent. The selected concentrations of (H_2O_2) (1.23, 2.23, and 3.23 vol.%) were chosen to cover the typical range of oxidant concentrations encountered in standard medical sterilization protocols. Furthermore, thermal effects at 37 °C were included to accelerate electrochemical kinetics at human body temperature (Table 2).

Table 2. Experimental matrix of immersion protocols and corrosive media conditions.

Protocol	Medium	H2O2 concentration [%]	Addition mode	Temperature [^{0}C]
TR0	3.5% NaCl	-	-	$25^{\pm3}$
TR1	3.5% NaCl + H_2O_2	1.25	Single dose (100µl of H_2O_2)	$25^{\pm2}$
TR2	3.5% NaCl + H_2O_2	2.23	Single dose (181µl of H_2O_2)	$25^{\pm2}$
TR3	3.5% NaCl + H_2O_2	3.23	Single dose (263µl of H_2O_2)	$25^{\pm3}$
TR4	3.5% NaCl + H_2O_2	1.23	Fractionated (4 x 25µl of H_2O_2)	$25^{\pm2}$
TR5	3.5% NaCl + H_2O_2	1,23	Single dose (100µl of H_2O_2)	$37^{\pm2}$
TR6	3.5% NaCl + H_2O_2	1,23	Fractionated (4 x 25µl of H_2O_2)	$37^{\pm2}$
TR6	3.5% NaCl + H_2O_2	1,23	Fractionated (4 x 25µl of H_2O_2)	

Specifically, for protocols TR04 and TR06, the oxidant was introduced via a fractionated addition (4 x 25µl of H_2O_2) rather than a single dose (100 µl). This sequential injection protocol was strategically designed to simulate dynamic medical sterilization cycles where oxidant levels are intermittently replenished, preventing stable repassivation of the chromium oxide layer and maintaining a high electrochemical potential at the metal-electrolyte interface.

The immersion duration was strictly maintained at 20 days for all batches. This timeframe was selected based on preliminary monitoring of the Open-Circuit Potential (OCP), which indicated that the transition from initial passive film degradation to detectable micro-pitting occurs within this period. This 20-day exposure effectively captures the critical early-stage structural degradation, allowing for a precise quantification of the synergistic effect between chloride ions, temperature, and oxidant replenishment on the material's yield strength.

2.5. Mechanical characterization: uniaxial tensile testing

Quasi-static uniaxial tensile tests were executed at the Strength of Materials Laboratory of the University of Jijel, Algeria, using a high-precision Zwick/Roell universal testing machine, which was fully interfaced with a microcomputer for real-time data acquisition and processing. To ensure statistical reliability and experimental consistency, standardized cylindrical specimens were evaluated across all batches (TR0 to TR06) at a controlled ambient temperature of 25 ± 2°C. A constant crosshead speed of 5 mm/min was maintained to rigorously capture the material's constitutive response, particularly during the elastoplastic transition. The investigation systematically quantified the evolution of critical mechanical properties, including the 0.2% offset yield strength (YS), the ultimate tensile strength (UTS), and the fracture stress. Furthermore, the elongation at break

(A %) was recorded as a primary indicator to evaluate the deleterious impact of the aggressive media on the material's ductility and work-hardening capacity.

2.6. Microhardness characterization

The surface mechanical resistance was evaluated using a Zwick/Roell Indentec digital microhardness tester to quantify the localized impact of the corrosive media on the material's integrity. To ensure statistical reliability and capture the mechanical evolution along the gauge length, five indentations were systematically performed on each specimen to calculate the average Vickers hardness (HV) and the corresponding standard deviation.

Measurements were conducted on the as-received material (TR0) and on all batches (TR01–TR06) following environmental exposure. After removal from the aggressive solutions, the specimens were gently rinsed with deionized water and dried with a high-pressure air dryer. This cleaning procedure was essential to remove residual electrolytes and protect the diamond indenter, while deliberately preserving the corrosion-induced surface modifications without any subsequent abrasive polishing.

In accordance with ISO 6507-1, a diamond pyramidal indenter was utilized with a 0.3 kgf load and a 15-second dwell time. The indentations were distributed directly along the external longitudinal surface of the cylindrical specimens to establish a quantitative correlation between the synergistic effect of Cl^-/H_2O_2 and the localized surface mechanical evolution of the AISI 304 alloy.

3. Results and discussion

3.1. Microstructural characterization

The as-received metallurgical state of the AISI 304 stainless steel was examined to establish a baseline for the subsequent mechanical evaluations, as illustrated in figure 2.

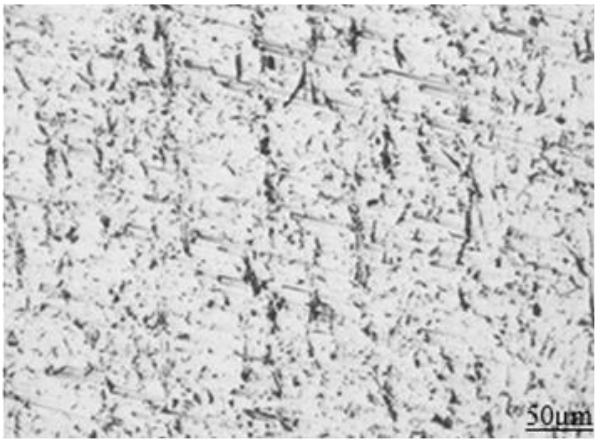

Figure 2. Optical micrograph of the as-received AISI 304 stainless steel showing equiaxed austenitic grains

The microstructure exhibits a characteristic austenitic configuration. The optical micrograph reveals a well-defined distribution of equiaxed grains, with the presence of numerous annealing twins, which are typical for face-centered cubic (FCC) alloys. This structural homogeneity is critical, as it ensures isotropic mechanical properties during uniaxial tensile deformation and provides a stable substrate for the formation of the chromium-oxide passive film [19]. No significant secondary phases, such

as δ-ferrite or large non-metallic inclusions, were observed, confirming the high metallurgical cleanliness of the alloy [20].

Recent investigations on the metallurgy of AISI 304 highlight that this type of stabilized austenitic matrix, characterized by coherent twin boundaries, is essential for maintaining high fracture toughness and work-hardening capacity [21]. Furthermore, the absence of chromium carbide ($M_{23}C_6$) precipitates at the grain boundaries indicates that the material is in a fully solution-annealed state [22]. This initial microstructural integrity confirms that the specimens are free from pre-existing metallurgical defects or sensitization, providing a rigorous starting point for the environmental exposure tests [23].

3.2. Surface integrity and micro-pitting morphometry

The localized mechanical resistance of the AISI 304 surgical steel was quantified through Vickers microhardness measurements. Five independent indentations were performed on each specimen to ensure statistical representativeness. The experimental results reveal an average baseline microhardness of 383.14 ± 0.87 HV. This relatively high value indicates a significant degree of prior work-hardening induced during manufacturing, which is essential for maintaining the sharpness and structural rigidity of surgical instruments [24].

Following the 20-day environmental exposure, a systematic degradation of surface hardness was recorded across all batches (Table 2).

The graphical evolution in Figure 3 illustrates a clear monotonic decrease in microhardness as environmental aggressiveness increases. A nearly linear downward trend is observed as the hydrogen peroxide concentration rises from 1.25% to 3.23% (TR01 to TR03), indicating a direct correlation between oxidant density and the progressive destabilization of the passive film.

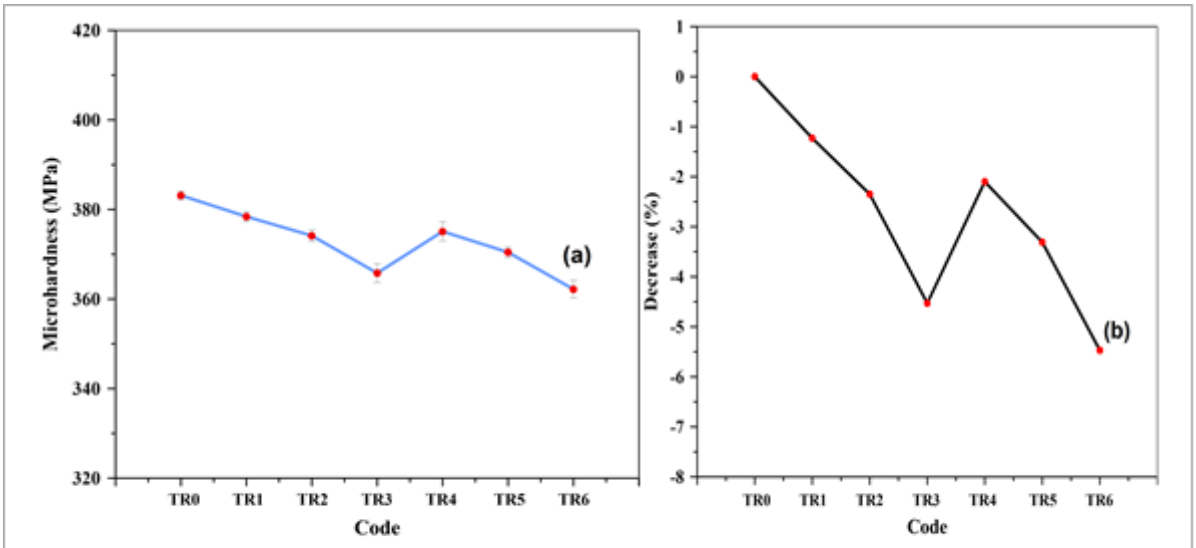

Figure 3. Vickers microhardness of AIS 304: (a) absolute values and (b) percentage decrease, following H_2O_2 concentration and immersion protocols at 25 °C and 37 °C.

Notably, the slope of the curve becomes significantly steeper for the fractionated addition protocols (TR04 and TR06). This behavior demonstrates that the frequency of chemical

replenishment, simulating repeated sterilization cycles, is more deleterious to surface integrity than cumulative concentration alone, effectively preventing stable repassivation. The most pronounced reduction occurred in the TR06 protocol (3.5% NaCl + fractionated H_2O_2 at 37 °C), where the microhardness dropped to 362.20 $^{\pm 1.98}$ HV, representing a 5.47% loss.

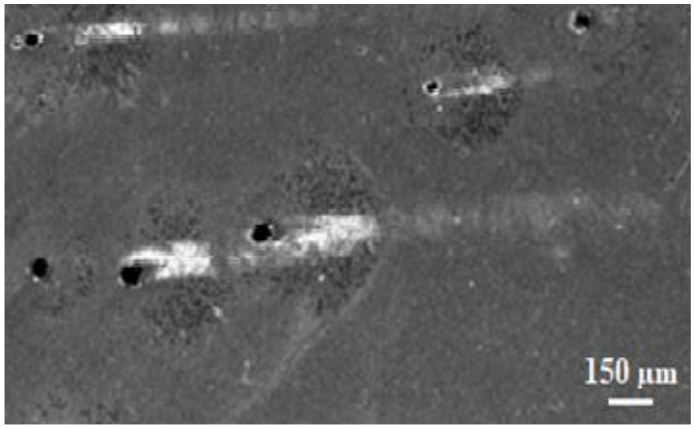

Figure 4. Optical micrograph of the as-received AISI 304 stainless steel showing equiaxed austenitic grains

This surface softening is visually confirmed by Scanning Electron Microscopy (SEM) analysis, which reveals significant localized damage. As illustrated in Figure 4, the specimen surface exhibits well-defined micro-pits with diameters ranging typically between 40 and 75 µm. From a fracture mechanics perspective, these pits act as geometric stress concentrators that reduce the effective load-bearing cross-section.

The thermal acceleration at 37 °C (human body temperature) induces a distinct downward shift of the entire profile, enhancing ionic diffusion kinetics through the oxide scale. In the context of reusable medical devices, such degradation is critical; pits of this magnitude can harbor biological contaminants, compromising the sterility of the instrument, while simultaneously triggering metallic ion release and compromising the precision of fine-edged tools like retractors or scissors [25–27].

3.3. Tensile test results and mechanical properties of surgical steel

The superposition of the engineering stress-strain curves (Figure 5) highlights a discernible modification in the mechanical response of the AISI 304 stainless steel when transitioned from ambient air (TR0) to the various aggressive electrolytic solutions (TR01–TR06).

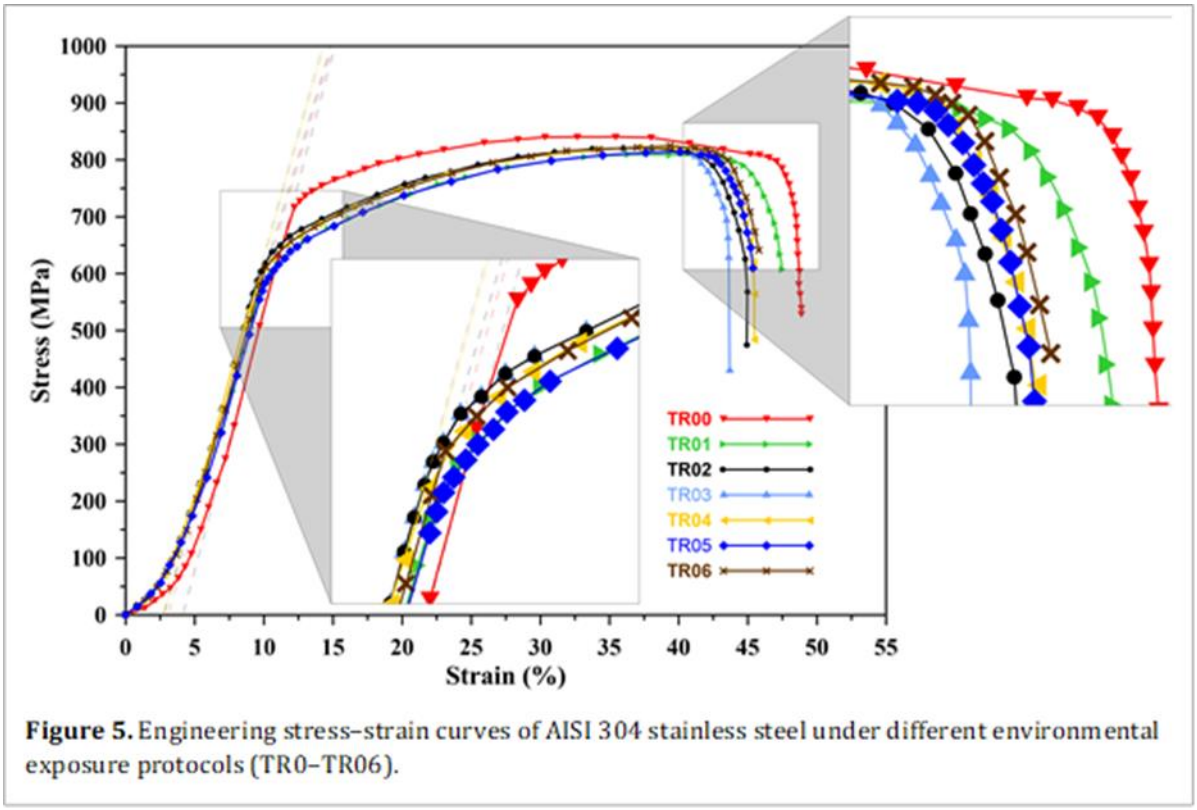

Figure 5. Engineering stress–strain curves of AISI 304 stainless steel under different environmental exposure protocols (TR0–TR06).

The comprehensive mechanical characteristics extracted from these tests, representing the structural integrity of the material under simulated clinical stress, are summarized in Table 3.

Table 3. Mechanical properties of AISI 304 stainless steel under different environmental exposure protocols.

Protocol	Yield strength (MPa)	Ultimate strength (MPa)	Stress at break (MPa)	Elongation (%)
TR0	**708.61**	**848.80**	**550.43**	**48.80**
TR1	**593.73**	**818.41**	**545.26**	**47.5**
TR2	585.24	815.01	542.51	45.20
TR3	**572.46**	**810.20**	**428.52**	**43.10**
TR4	591.07	813.5	540.81	44.75
TR5	580.61	812.02	535.09	44.50
TR6	**565.82**	**805.50**	520.22	43.40

The experimental results reveal that the yield strength (YS) is the most sensitive parameter to environmental exposure [28, 29]. While the as-received material (TR0) exhibits a high YS of 708.6 MPa due to the prior cold-drawing process (essential for the stiffness of surgical tools), a significant degradation is observed in all corrosive batches [30]. Specifically, the YS dropped to 593.7 MPa in the TR1 condition, representing a loss of nearly 16.2%. In contrast, the ultimate tensile strength (UTS) remained relatively stable. This preferential attack on the elastic limit suggests that the synergy between Cl^- ions and H_2O_2 promotes the formation of sub-surface micro-defects and hydrogen

absorption, facilitating early dislocation movement and plastic flow before the macroscopic structural capacity is reached [32].

Interestingly, increasing the H_2O_2 concentration (TR2 and TR3) or adding it fractionally (TR4 and TR6) led to a progressive and significant decline in YS, reaching its minimum at 565.8 MPa under the TR6 protocol [31]. This continuous degradation indicates that the synergistic interaction between temperature (37 °C) and constant oxidant replenishment prevents the formation of a stable protective layer, maintaining high pit growth kinetics [28, 31]. Furthermore, the systematic reduction in elongation at break, reaching its lowest values in TR3 (43.10%) and TR6 (43.40%), confirms a deleterious loss in ductility [33]. In a clinical context, such a reduction in ductility combined with localized stress concentrations from pitting acts as a precursor for premature fracture of reusable medical devices under operative loads [34, 35].

3.3. Analysis of mechanical property variations and clinical reliability

The macroscopic mechanical response of the AISI 304 surgical steel exhibits a clear dependence on the synergistic interaction between the physiological environment and the material's microstructural state. The data extracted from the engineering stress-strain curves (table 3) are graphically analyzed to evaluate the structural integrity of high-precision instruments under simulated operative stress.

3.3.1. Evolution of yield strength and ultimate strength

The variation of yield strength (YS) across the protocols (figure 6 a) represents the most critical finding for surgical applications.

Compared to the control (708.6 MPa), the YS shows a significant and continuous decline, reaching its minimum at 565.8 MPa under the TR6 protocol. This steady degradation suggests that the initial synergy between Cl^- ions and H_2O_2 promotes the formation of sub-surface micro-defects that facilitate early dislocation movement. According to the Adsorption-Induced Dislocation Emission (AIDE) mechanism, the presence of aggressive species at surface defects lowers the energy barrier for dislocation nucleation [36-37]. For a surgeon, this reduction is critical; it implies that instruments such as orthopedic drills or hemostatic forceps could undergo permanent plastic deformation at loads between 16.2% and 20.2% lower than their nominal design, potentially compromising surgical precision and patient safety [38].

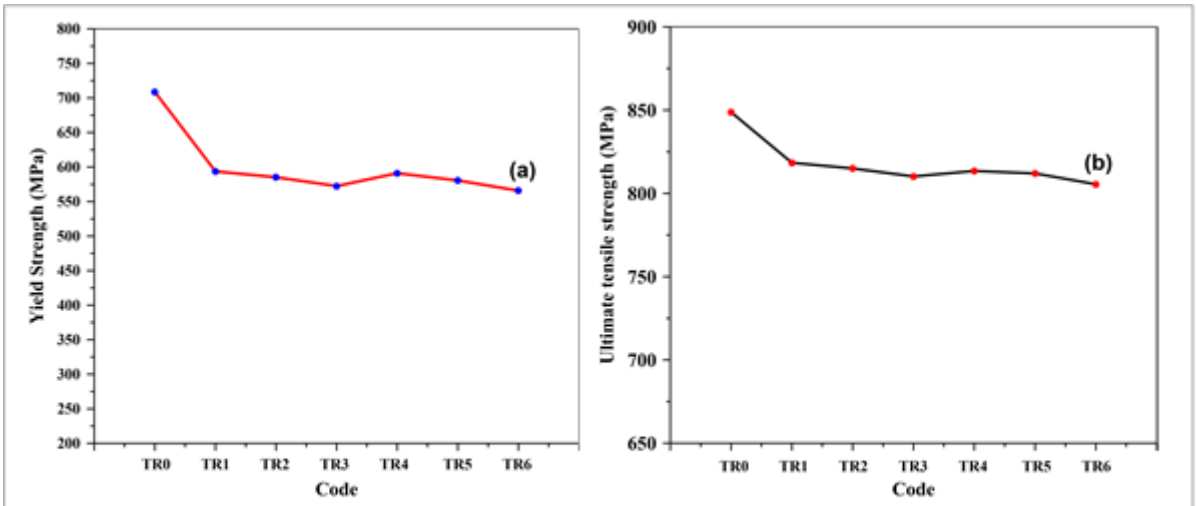

Figure 6. Tensile properties of AISI 304 as a function of the aggressive medium: (a) yield strength and (b) ultimate tensile strength (UTS).

In contrast, the ultimate tensile strength (UTS) variation (figure 6b) remains relatively stable, hovering between 805 and 818 MPa for all corrosive batches.

This demonstrates that while the environmental impact is severe during the elastic-plastic transition, the bulk load-bearing capacity is less affected. However, this differential sensitivity represents a "silent" clinical danger: an instrument may appear structurally intact while its functional geometry is already compromised by yielding during high-load procedures [39-40].

3.3.2. Variation of fracture stress and elongation

The deleterious impact on ductility is evidenced by the variation of elongation at break (figure 7a) and fracture stress (figure 7b).

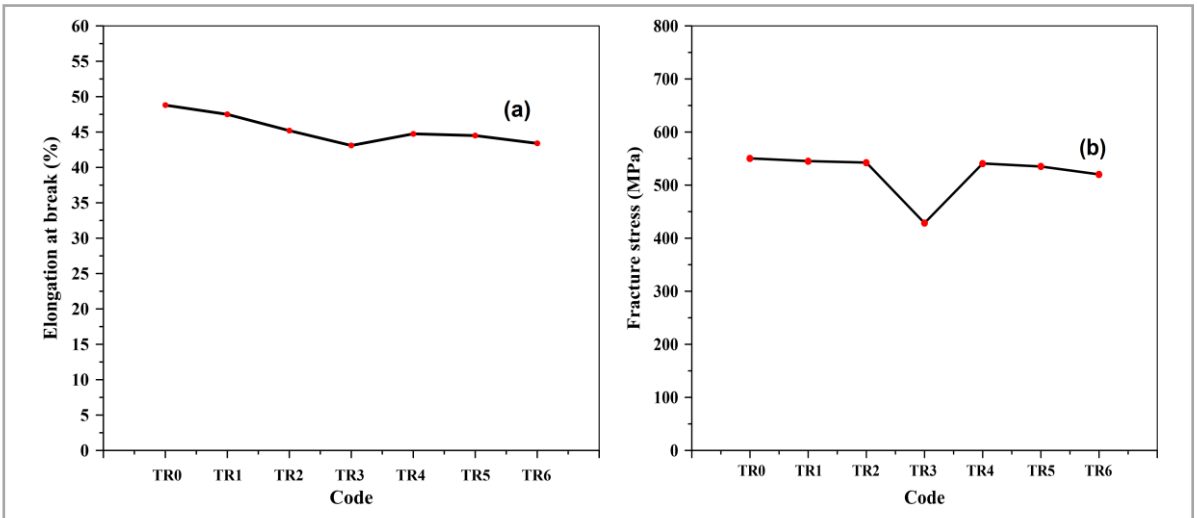

Figure 7. Tensile ductility parameters of AISI 304 under environmental aggressiveness: (a) elongation at break (%) and (b) fracture stress.

The minimum elongation recorded (43.10% in TR3) serves as a hallmark of Environmentally Assisted Cracking (EAC), where the synergy between chemical aggression and mechanical loading

triggers premature failure. In clinical settings, localized pitting acts as a potent geometric stress concentrator, altering the local stress state from uniaxial to triaxial, thereby accelerating the transition from uniform plastic deformation to localized crack initiation [41].

Furthermore, sequential oxidant replenishment (TR4 and TR6), simulating repeated sterilization cycles, induces a state of transient passivity where the stable film reformation is constantly interrupted. At the 37 °C thermal threshold, molecular kinetics are significantly enhanced, acting as a kinetic multiplier for both ionic diffusion and the cathodic reduction of H_2O_2, which promotes hydrogen absorption into the austenitic lattice [42]. Once trapped within the lattice, the interaction between hydrogen-related species and dislocation mobility at the crack tip promotes localized slip and decohesion (HELP/HEDE mechanisms), further exacerbating the material's vulnerability [43].

In a surgical context, this combined loss of yield strength and ductility acts as a direct precursor for the catastrophic fracture of reusable medical devices under complex operative loads. These findings necessitate rigorous life-cycle assessments based on sterilization frequency and biochemical exposure history to ensure that instruments maintain their mechanical reliability throughout their clinical service life

4. Conclusion

The present investigation provides a rigorous quantitative evaluation of the environmental degradation of AISI 304 surgical stainless steel under complex oxidative-saline exposure, simulating the aggressive conditions of physiological fluids and chemical sterilization protocols. By integrating high-precision uniaxial tensile testing with microstructural and surface characterization, the following conclusions were established regarding the material's structural integrity:

(1) Microstructural analysis confirmed a stable austenitic matrix with a high density of annealing twins, essential for the dimensional stability of surgical tools. The elevated baseline microhardness (383.14 HV) and yield strength (708.6 MPa) confirm a significant prior strain-hardening state. While providing superior initial stiffness, this condition also accelerates localized chemical attacks due to high dislocation density.

(2) The study highlights the preferential susceptibility of the Yield Strength (YS) to corrosive media. A substantial drop of 115 to 143 MPa was recorded compared to the control. The most severe loss occurred under the TR6 protocol (565.8 MPa), which combines thermal activation (37 °C) and fractionated oxidant replenishment. This demonstrates that the frequency of disinfection cycles at body temperature is more decisive in destabilizing the protective film than the chemical concentration alone.

(3) While the ultimate load-bearing capacity remained relatively stable, a deleterious loss in ductility was observed. The elongation at break dropped to a critical minimum of 43.10% (TR3) and 43.40% (TR6). This identifies a clinical safety threshold where localized pitting facilitates premature crack initiation, increasing the risk of catastrophic fracture during operative procedures.

(4) Even a short-term exposure of 20 days significantly impairs the mechanical reliability of reusable medical devices. The synergy between chloride ions, thermal activation at 37 °C, and intermittent oxidation (H_2O_2) compromises the safety margins of AISI 304 instruments. These results are

essential for developing life-cycle management protocols and ensuring the structural reliability of surgical hardware in modern clinical scenarios.

Conflicts of Interest

The authors declare no conflict of interest.

Data Availability Statement

The data that support the findings of this study are available from the corresponding author upon reasonable request.

Ethics Statement

Not applicable. This study does not involve human participants or animals.

Funding Statement

This research did not receive any specific grant from funding agencies in the public, commercial, or not-for-profit sectors.

Acknowledgements

The authors would like to express their gratitude to the BCR National Enterprise, specifically the units of Bordj Menaïel (Boumerdès, Algeria) and Aïn Kebira (Sétif, Algeria), for providing the AISI 304 austenitic stainless steel raw materials. Special thanks are also extended to the Mechanical Construction Company of Khenchela (MCCK, Algeria) for their technical support in the high-precision CNC fabrication of the specimens. The authors also acknowledge the Mechanical Laboratory of the University of Jijel (Algeria) and the Public Hospital Establishment (EPH) of Batna (Algeria) for their valuable contribution to the experimental investigation and for providing the clinical context for the surgical instruments' integrity study.

References

[1] Paiva J M, Amorim H J, Junior A M, Silva R B, Costa C A and Ferreira J S 2021 *Materials* 14 3120
[2] Zhang L C and Chen L Y 2019 *Bioact. Mater.* 4 322
[3] Niinomi M, Nakai M and Hieda J 2022 *Metallic biomaterials for surgical instrumentation* (Advances in Metallic Biomaterials) (Springer) p 15
[4] Kumar S, Maheshwari S and Sharma A 2023 *J. Alloys Compd.* 935 168120
[5] Pardo A, Merino M C, Coy A E, Viejo F, Arrabal R and Feliu S 2020 *Corros. Sci.* 165 108391
[6] Rossi F, Casati R and Vedani M 2024 *Mater. Sci. Eng.* A 890 145920
[7] Wang T, Zhang S and Li J 2022 *Mater. Des.* 215 110432
[8] Al-Sultani H A, Al-Rubaiey H and Al-Amiery A A 2023 *Appl. Surf. Sci.* 610 155512
[9] Yahia L, Nouicer E and Benlahreche F Z 2021 *Defect Diffusion Forum* 406 145
[10] Singh R, Kumar A and Dahotre N B 2021 *Mater. Today: Proc.* 45 4821
[11] Shahzad M A, Cha J H and Kim J G 2022 *Corros. Sci.* 195 109968

[12] Rodriguez J, Fernandez J and Lopez M 2020 *Electrochim. Acta* 340 135987
[13] Zhang H, Li Y and Wang J 2023 *J. Bio- Tribo-Corros.* 9 24
[14] Ahmed Y M, El-Sabbagh A M and Soliman M S 2022 *J. Mech. Behav. Biomed. Mater.* 126 105014
[15] Benyounis K Y, Olabi A G and Hashmi M S 2020 *J. Mater. Process. Technol.* 278 116521
[16] Jelinek P, Kasparek J and Vlach F 2021 *Corros. Rev.* 39 315
[17] Lynch S 2019 *Corros. Rev.* 37 373
[18] ISO 7153-1 2016 *Surgical instruments — Materials — Part 1: Metals* (International Organization for Standardization)
[19] Rivolta B, Gerosa R and Tassan M 2021 *Metall. Mater. Trans.* A 52 1102
[20] Lothongkum G, Viyanit E and Chuchumpol P 2022 *Mater. Charact.* 184 111680
[21] Wang X G, Wang Z and Zhang J 2023 *Surf. Coat. Technol.* 452 129110
[22] Huang C J, Lin X and Feng J 2024 *J. Iron Steel Res. Int.* 31 150
[23] Moayed M S, Khalesi H and Karimi M 2020 *Corros. Sci.* 170 108661
[24] Benyounis K Y, Hashmi M S and Olabi A G 2020 *J. Mater. Process. Technol.* 278 116521
[25] Shahzad M A, Kim J G and Cha J H 2022 *Corros. Sci.* 195 109968
[26] Zhang L C and Chen L Y 2019 *Bioact. Mater.* 4 322
[27] Singh R, Kumar A and Dahotre N B 2021 *Mater. Today: Proc.* 45 4821
[28] Al-Sultani H A, Al-Rubaiey H and Al-Amiery A A 2023 *Appl. Surf. Sci.* 610 155512
[29] Rodriguez J, Fernandez J and Lopez M 2020 *Electrochim. Acta* 340 135987
[30] Wang T, Zhang S and Li J 2022 *Mater. Des.* 215 110432
[31] Jelinek P, Kasparek J and Vlach F 2021 *Corros. Rev.* 39 315
[32] Kumar S, Maheshwari S and Sharma A 2023 *Int. J. Plasticity* 160 103482
[33] Ahmed Y M, El-Sabbagh A M and Soliman M S 2022 *J. Mech. Behav. Biomed. Mater.* 126 105014
[34] Rossi F, Casati R and Vedani M 2024 *Mater. Sci. Eng.* A 890 145920
[35] Paiva J M, Amorim H J and Ferreira J S 2021 *Materials* 14 3120
[36] Lynch S 2019 *Corros. Rev.* 37 373
[37] Zhang H, Li Y and Wang J 2023 *J. Bio- Tribo-Corros.* 9 24
[38] Prasannavenkatesan R, Kumar S and Singh R 2022 *J. Mech. Behav. Biomed. Mater.* 128 105120
[39] Rossi F, Casati R and Vedani M 2024 *Mater. Sci. Eng.* A 890 145920
[40] Ahmed Y M, El-Sabbagh A M and Soliman M S 2022 *J. Mech. Behav. Biomed. Mater.* 126 105014
[41] Kumar S, Maheshwari S and Sharma A 2023 *Int. J. Plasticity* 160 103482
[42] Wang T, Zhang S and Li J 2022 *Mater. Des.* 215 110432
[43] Zhang H, Li Y and Wang J 2023 *Corros. Sci.* 212 110901